FDTD Simulation of Relaxation Oscillation and the Lasing Mode of a Photonic-Crystal Laser

G. Hugh Song,[a] Soan Kim,[a] Kyu Hwan Hwang,[a] and Kyo-Bang Chung[b]

[a]Kwangju Institute Science & Technology, Buk-gu, Gwangju, Korea
[b]Hongik Univ., Seoul, Korea

ABSTRACT

We have developed an finite-difference time-domain program that can analyze photonic devices with gain and/or dispersion. As an example, a two-dimensional photonic-crystal laser is simulated. The simulation can show the relaxation oscillation behavior at extremely high current injection.

Keywords: FDTD, finite-difference time-domain analysis, photonic crystal lasers

1. INTRODUCTION

Recently, application of the finite-difference time-domain (FDTD) analysis[1] to various engineering problems is becoming practical owing to remarkable development of high-speed computers. The need for such a program in the analysis of photonic-crystal devices is especially recognized in that the capability of other conventional techniques such as the beam-propagation analysis and various types of frequency-domain analysis is seriously limited for the purpose.

Among many photonic-crystal devices, photonic-crystal lasers[2] attracted a considerable attention because the capability of such devices is not yet fully investigated since they have not been made close to perfection. Unlike conventional semiconductor lasers including vertical-cavity lasers, distributed-feedback (DFB) lasers, and distributed-Bragg-reflection (DBR) lasers, analysis of photonic-crystal lasers is relatively difficult because of their inherent fully-three-dimensional characteristics and their quite complicated modal and polarization characteristics. A considerable amount of research[3,4] is being carried on two-dimensional photonic-crystal lasers formed on a slab-waveguide of half-wavelength width. Design of the structure is made mostly with the operating principle of DBR in mind.

In this paper, we report on the development of a FDTD simulator which can analyze such photonic-crystal lasers. The gain medium is modeled by a region of an inverted carrier-density with the generalized Lorentz-dispersion characteristics. The regions for dispersive media and the perfectly-matched layers (PML's) are fully integrated in the code for full parallelization and efficient memory handling. For such a purpose, layers of anisotropically dispersive electric/magnetic media[5] are introduced in all computation boundaries, while the recursive-convolution method[6] with the piecewise-constant approximation[7] has been used for simulation of both the dispersive media and the PML layers. We have found that this combination allows the most efficient coding and memory usage amenable to parallelization.

The discretized standard rate equation for the evolution of the electron density is solved together at each FDTD time-stepping. This should enable accurate analysis of the relaxation oscillation of emitted optical power of the laser. Both a fully three-dimensional version as well as the two-dimensional version of the simulator are developed simultaneously with almost all components of the code shared between the two versions. However, it must be mentioned that, due to limitation of the available computer resources, the results shown in this paper have been mostly obtained with the two-dimensional version from the time-scaled-down simulation by adjusting the carrier lifetime.

Send correspondence to G.H.S.: E-mail: ghsong@kjist.ac.kr, Telephone: +82-62-970-2210, Address: KJIST, Dept. of Info. & Commun., Buk-gu, Gwangju, Korea 500-712

Photonic Bandgap Materials and Devices, Ali Adibi, Axel Scherer, Shawn-Yu Lin, Editors,
Proceedings of SPIE Vol. 4655 (2002) © 2002 SPIE · 0277-786X/02/$15.00

2. THE FINITE-DIFFERENCE TIME-DOMAIN METHOD WITH DISPERSION

We simulate the four Maxwell equations

$$\boldsymbol{\nabla} \cdot \hat{\varepsilon}(\boldsymbol{r}, \omega)\, \boldsymbol{E} = 0, \tag{1}$$

$$\boldsymbol{\nabla} \cdot \hat{\boldsymbol{\mu}}(\boldsymbol{r}, \omega)\, \boldsymbol{H} = 0, \tag{2}$$

$$\boldsymbol{\nabla} \times \boldsymbol{E} = \mathrm{i}\,\omega\, \hat{\boldsymbol{\mu}}(\boldsymbol{r}, \omega)\, \boldsymbol{H}, \tag{3}$$

$$\boldsymbol{\nabla} \times \boldsymbol{H} = -\mathrm{i}\,\omega\, \hat{\varepsilon}(\boldsymbol{r}, \omega)\, \boldsymbol{E}, \tag{4}$$

with the generalized electric permittivity tensor $\hat{\varepsilon}(\boldsymbol{r}, \omega)$ and the magnetic permeability tensor $\hat{\boldsymbol{\mu}}(\boldsymbol{r}, \omega)$ with a certain type of frequency dependence. The two material tensors are "generalized" in the sense that

$$\frac{\partial \hat{\boldsymbol{D}}(\boldsymbol{r}, t)}{\partial t} \equiv \int_{-\infty}^{\infty} [\boldsymbol{J}(\boldsymbol{r}, \omega) - \mathrm{i}\,\omega\, \boldsymbol{D}(\boldsymbol{r}, \omega)] \exp(-\mathrm{i}\,\omega\, t)\, \frac{\mathrm{d}\omega}{2\,\pi} \equiv -\int_{-\infty}^{\infty} \mathrm{i}\,\omega\, \hat{\varepsilon}(\omega)\, \boldsymbol{E}(\boldsymbol{r}, \omega)\, \frac{\mathrm{d}\omega}{2\,\pi}. \tag{5}$$

where $\boldsymbol{J}(\boldsymbol{r}, \omega)$ refers to the current density due to motion of free carriers.

In the PML, according to the algorithm of perfectly-matched anisotropic layers,[5] the electric permittivity and the magnetic permeability are expressed as

$$\hat{\varepsilon}(\boldsymbol{r}, \omega) = \varepsilon(\infty)\, \boldsymbol{\Lambda}(\boldsymbol{r}, \omega), \qquad \hat{\boldsymbol{\mu}}(\boldsymbol{r}, \omega) \equiv \begin{cases} \mu_0\, \boldsymbol{\Lambda}(\boldsymbol{r}, \omega), & \text{in the PML,} \\ \mu_0, & \text{in the inner dispersive region,} \end{cases} \tag{6}$$

where the tensor factor of a diagonal matrix $\boldsymbol{\Lambda}(\boldsymbol{r}, \omega)$ is shared in the PML between the electric permittivity and the magnetic permeability. The lth diagonal element can be expressed as

$$\Lambda_{ll}(\boldsymbol{r}, \omega) \equiv \left[1 + \sum_{p=1}^{M_l} \frac{\Gamma_l^{(p)}}{-\mathrm{i}\,\omega - s_l^{(p)}} + \frac{Q_l}{-\omega^2}\right], \qquad l = \mathrm{x},\, \mathrm{y},\, \mathrm{z}, \tag{7}$$

where M_l is the order of the rational function in the region containing the position denoted by $\boldsymbol{r}$.

In the inner region of dispersion, the three diagonal elements are basically the same, which represents an isotropic material of dispersion with gain or loss. All the poles, other than the ones on the imaginary axis of the complex-ω plane, should exist in pairs, so that the simplest implementation of the gain medium is modeled as the electric susceptibility function of

$$\chi(\omega) \equiv \sum_{q=1}^{N} \left[\frac{\Gamma^{(q)}}{-\mathrm{i}\,\omega - s^{(q)}} + \frac{\Gamma^{(q)*}}{-\mathrm{i}\,\omega - s^{(q)*}}\right]. \tag{8}$$

where N is the reduced number of terms from M_l owing to the pole pairs for every Lorentzian function in the summation. The poles and residues are represented to the resonance frequencies ω_q and the damping constants γ_q by

$$s^{(q)} = -\gamma_q + \mathrm{i}\,\omega_q, \tag{9}$$

$$\Gamma^{(q)} = \frac{\varepsilon(0) - \varepsilon(\infty)}{\varepsilon_0}\, \frac{f_q\, \omega_q}{\mathrm{i}\,2}, \tag{10}$$

where f_q is the oscillator strength which is related to the carrier density in the active region of the semiconductor medium. Unlike the true physical permittivity function of ω with $\hat{\varepsilon}_{ll}(\infty) = \varepsilon_0$, we choose the value of $\hat{\varepsilon}_{ll}(\infty)$ properly at a sufficiently high frequency, so that the variation of $\hat{\varepsilon}(\omega)$ is adequately represented in the range of frequencies under consideration.

The dispersive material is implemented by implementing the inverse Fourier transform of the permittivity tensor function of ω in Eq. (4) by

$$\check{\varepsilon}_{ll}(t) \equiv \int_{-\infty}^{\infty} \hat{\varepsilon}(\omega)\, \Lambda_{ll}(\boldsymbol{r},\, \omega) \exp(-\mathrm{i}\,\omega\, t)\, \frac{\mathrm{d}\omega}{2\,\pi} \equiv \hat{\varepsilon}_{ll}(\infty) \left[\delta(t) + \sum_{q\,=\,1}^{N_l} \mathrm{Re}\, \check{\chi}_l^{(q)}(t)\right], \tag{11}$$

$$\check{\chi}_l^{(q)}(t) \equiv R_l^{(q)}\, \theta(t) \exp(s_l^{(q)}\, t), \tag{12}$$

where $\theta(t)$ is the Heaviside step function. We now apply the piecewise-constant recursive convolution technique which was first introduced in a paper by Schuster, et al..[7] Formulas suitable for numerical implementation are rewritten as

$$\left[\frac{1}{\Delta t} + \sum_{q\,=\,1}^{N_l} \mathrm{Re}\, \check{\chi}_l^{(q)}|_0^{1/2}\right] \mathcal{E}_l|^{n\,+\,1} = \left[\frac{1}{\Delta t} - \sum_{q\,=\,1}^{N_l} \mathrm{Re}\, \check{\chi}_l^{(q)}|_{-1/2}^{0}\right] \mathcal{E}_l|^{n} - \left[\sum_{q\,=\,1}^{N_l} \mathrm{Re}\left\{\left[1 - \mathrm{e}^{-s_l^{(q)}\,\Delta t}\right] \Phi_l^{(q)}|^{n\,+\,1}\right\} + Q_l\, I_l|^{n\,+\,1/2}\right] + \frac{[\boldsymbol{\nabla} \times \boldsymbol{\mathcal{H}}]_l\,|^{n\,+\,1/2}}{\hat{\varepsilon}_{ll}(\infty)}. \tag{13}$$

where Δt is the width of the time step in the FDTD simulation. The above relation along with

$$\Phi_l^{(q)}|^{n+1} = \left\{\left[\check{\chi}_l^{(q)}|_0^{1/2} + \check{\chi}_l^{(q)}|_{-1/2}^{0}\right] \mathcal{E}_l|^{n} + \Phi_l^{(q)}|^{n}\right\} \exp(s_l^{(q)}\, \Delta t), \tag{14}$$

$$I_l|^{n\,+\,1/2} = I_l|^{n\,-\,1/2} + \Delta t\; \mathcal{E}_l|^{n}, \tag{15}$$

$$\check{\chi}_l^{(q)}|_0^{1/2} = \Gamma_l^{(q)}\, \mathrm{exprl}\Big(s_l^{(q)}\, \Delta t/2\Big), \tag{16}$$

$$\check{\chi}_l^{(q)}|_{-1/2}^{0} = \Gamma_l^{(q)}\, \mathrm{exprl}\Big(-s_l^{(q)}\, \Delta t/2\Big), \tag{17}$$

where $\mathrm{exprl}\, z \equiv [\exp z - 1]\,/z$, provides the needed algorithm which is amenable to a systematic treatment of the dispersive material in FDTD simulations.

3. MODEL FOR THE GAIN MEDIUM AND THE POPULATION INVERSION

The gain-dispersion characteristics of the active semiconductor medium are modeled by the Lorentzian formula of Eq. (8) with a single pair of poles. For the simulation of the gain medium, we performed an "experimental" fit between location of the poles and the carrier density of in the active region to obtain its relation to the numbers for γ_1 and ω_1.

Beside the amplification of the propagating light which is present in the medium, there exists spontaneous emission which actually provides the seed for the amplifying light in the medium. Such emission of light is modeled by a randomly oriented polarization current density with the magnitude properly determined in each cell of the FDTD model. These two sources of light generation can be implemented in the FDTD simulator, once each module is properly prepared.

Similar to the dynamic simulator of a semiconductor laser based on the analysis of resonance modes, we need a rate equation which updates the number of carriers inside the active region. The equation can be obtained by considering the classical theorem of Poynting in regard to the energy balance. According to the theorem,

$$\boldsymbol{\nabla} \cdot \boldsymbol{\mathcal{E}}^{1} \times \boldsymbol{\mathcal{H}}^{1} + \frac{\mu_0}{2}\, \frac{\partial}{\partial t} \boldsymbol{\mathcal{H}}^{1} \cdot \boldsymbol{\mathcal{H}}^{1} + \frac{\varepsilon(\infty)}{2}\, \frac{\partial}{\partial t} \boldsymbol{\mathcal{E}}^{1} \cdot \boldsymbol{\mathcal{E}}^{1} + \boldsymbol{\mathcal{E}}^{1} \cdot \frac{\partial \hat{\boldsymbol{\mathcal{P}}}^{1}}{\partial t} = 0, \tag{18}$$

The polarization current $\partial \boldsymbol{\mathcal{P}}^{1}/\partial t$ in the last term of the left-hand side represents the interaction of the external field and the dipoles in a semiconductor active medium. This term is balanced with the energy which is provided

either by the injection current or by the pumping light. For the case of current injection, the rate equation can be written as

$$\iiint_V \boldsymbol{\mathcal{E}}^{\mathrm{l}} \cdot \frac{\partial \hat{\boldsymbol{\mathcal{P}}}^{\mathrm{l}}(\boldsymbol{r},\, t)}{\partial t}\, \mathrm{d}^3\boldsymbol{r} - \hbar\, \omega_{\mathrm{l}} \left[\frac{\mathrm{d}N_{\mathrm{e}}(t)}{\mathrm{d}t} - \frac{I^{\mathrm{qs}}(t)}{q_{\mathrm{e}}} \right] = 0, \tag{19}$$

where

$$N_{\mathrm{e}}(t) \equiv \iiint_V n_{\mathrm{e}}(\boldsymbol{r},\, t)\, \mathrm{d}^3\boldsymbol{r} \tag{20}$$

is the total number of carriers in the active layer, and $I^{\mathrm{qs}}(t)$ is the injection current.

4. TWO-DIMENSIONAL SIMULATION RESULTS

From these considerations, we have performed a two-dimensional calculation on a structure which has become well-known from the publication of its structure in Science.[8] In the simulation, we assumed the case of current injection instead of optical pumping in their experiment. As mentioned previously, the choice of the two-dimensional simulator and the method of pumping is largely driven by the need in the development stage of the simulator which requires a tremendous amount of computer resources in terms of computing time and memory. We first tried to find the condition for the relaxation oscillation while we are finding the lasing optical mode. As expected from the known property[9] of the triangular lattice structure with a single defect made of a missing hole at the center, the lasing mode has been found to be the doubly-degenerate dipole-shaped field as shown in Fig. 1. The animation obtained from the simulator has shown that the axis of the dipole field is constantly rotating. It confirms that the mode is doubly-degenerate as the theory indicates.

The four plots of Fig. 2 show the familiar appearances at a certain level of current injection. The magnitude of the injected current is unrealistically large. The choice has been made to show the relaxation oscillation which has been regarded as the result of a typical semiconductor laser. At the practical level of either optical pumping or current injection, we carefully suggest that the microcavity laser of this kind will not show the relaxation oscillation behavior. At the time of writing this document, we have assumed a two-dimensional structure for the purpose of developing the simulator. The correct account on this relaxation behavior appears to be possible after a three-dimensional analysis in the near future.

5. SUMMARY

In summary, we developed the two-dimensional FDTD simulator which integrates the scheme of anisotropic PML's and the piecewise-constant approximation for recursive-convolution integral. With this new functionality of the simulator, we have been able to numerically create a situation for relaxation oscillation. The preliminary result suggests that the lasers of this kind will not show the typical relaxation oscillation except the initial overshoot of the light output at the initial turn-on time-delay. We hope that the full three-dimensional simulator clarifies this issue at the time of presentation.

ACKNOWLEDGMENTS

This work has been supported in part by the Institute of Information Technology Assessment through the CHOAN Program, by the Korea Science and Engineering Foundation through the UFON ERC Program, and by the Ministry of Education through the BK-21-IT Program.

REFERENCES

1. K. S. Yee, "Numerical solution of initial boundary value problems involving maxwell's equations in isotropic media," *IEEE Trans. Antennas Propagat.* **14**, pp. 302–307, 1966.
2. T. Baba, "Photonic crystals and microdisk cavities based on gainasp-inp system," *IEEE J. Sel. Topics on Quantum Electron.* **3**, pp. 808–830, 1997.
3. J. Vučković, O. Painter, Y. Xu, A. Yariv, and A. Scherer, "Finite-difference time-domain calculation of the spontaneous emission coupling factor in optical microcavities," *IEEE J. Quantum Electron.* **35**, pp. 1168–1175, 1997.

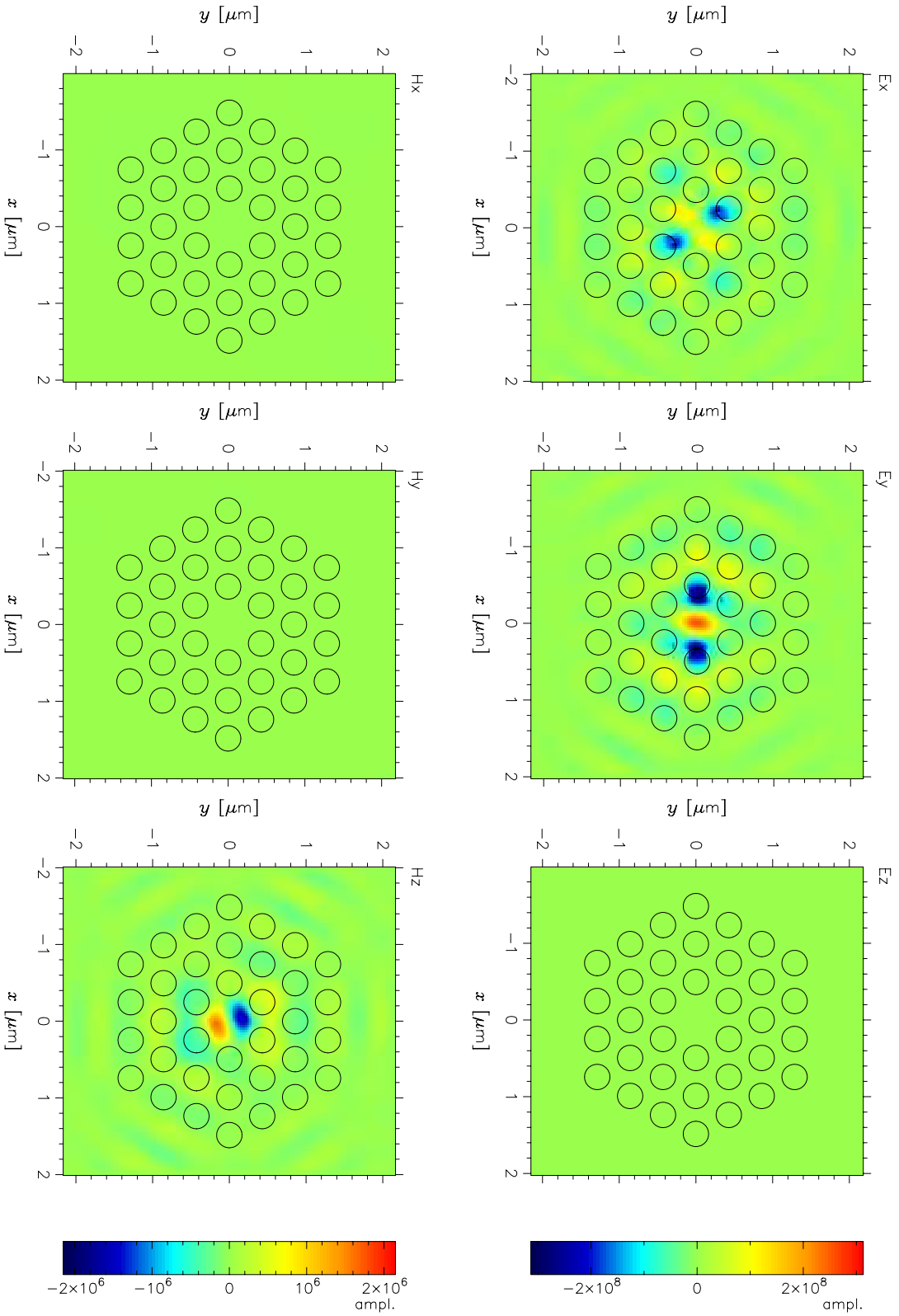

Figure 1. Simulated field profile of the lasing mode built-up in a photonic-crystal microcavity. The three plots in the right column show the snapshots of $\mathcal{E}_{\rm x}$, $\mathcal{E}_{\rm y}$, and $\mathcal{E}_{\rm z}$, while those of the left column show the snapshots of $\mathcal{H}_{\rm x}$, $\mathcal{H}_{\rm y}$, and $\mathcal{H}_{\rm z}$.

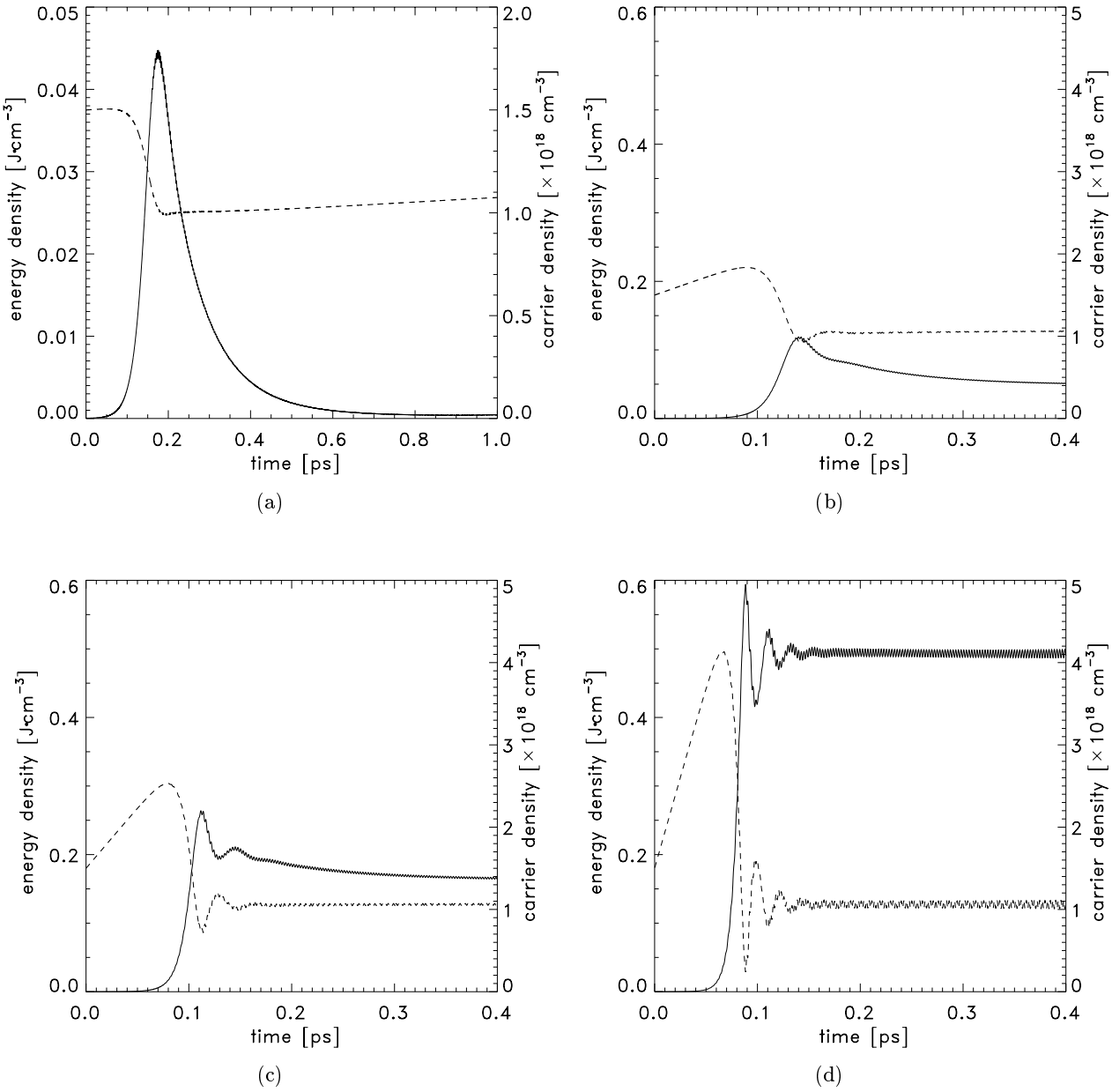

Figure 2. The relaxation oscillation behavior obtained from a two-dimensional simulator with the simulated currents of (a) 0.1 A, (b) 3 A, (c) 10 A, and (d) 30 A. The magnitudes of the injected current bear some inaccuracy from the limitation of the two-dimensional simulator. Solid lines represent the energy density of the cavity and the dashed curves represent the the carrier density in the active region of the semiconductor.

4. J. K. Hwang, H. Y. Ryu, D. S. Song, I. Y. Han, H. K. Park, D. H. Jang, and Y. H. Lee, "Continuous room-temperature operation of optically pumped two-dimensional photonic crystal lasers at 1.6 μm,," *IEEE Photonics Technol. Lett.* , pp. 1295–1297, 2000.
5. Z. S. Sacks, D. M. Kingsland, R. Lee, and J.-F. Lee, "A perfectly-matched anisotropic absorber for use as an absorbing boundary condition," *IEEE Trans. Antennas Propagat.* **43**, pp. 1460–1463, 1995.
6. R. J. Luebbers and F. Hunsperger, "FDTD for n-th-order dispersive media," *IEEE Trans. Antennas Propagat.* **21**, pp. 1087–1091, 1953.
7. J. Schuster and R. J. Luebbers, "An accurate algorithm for dispersive media using a piecewise constant recursive convolution technique," *IEEE Antennas and Propagation Soc. Internat. Symp. Digest* , pp. 2018–2021, 1998.
8. O. Painter, R. K. Lee, A. Yariv, A. Scherer, J. D. O'Brien, P. D. Dapkus, and I. Kim, "Two-dimensional photonic bandgap defect mode laser," *Science* **284**, p. 1819, 1999.
9. K. Sakoda, *Optical Properties of Photonic Crystals*, Springer, Berlin, 2001.